10.1098/rsta.2002.1080

THE ROYAL SOCIETY

Mantle-circulation models with sequential data assimilation: inferring present-day mantle structure from plate-motion histories

By Hans-Peter Bunge[1], M. A. Richards[2] and J. R. Baumgardner[3]

[1] *Department of Geosciences, Princeton University, Princeton, NJ 08544, USA* (bunge@princeton.edu)

[2] *Department of Earth and Planetary Sciences, University of California, Berkeley, Berkeley, CA 94720, USA* (markr@seismo.berkeley.edu)

[3] *T-Division, Los Alamos National Laboratory, Los Alamos, NM 87545, USA* (johnrb@lanl.gov)

Published online 27 September 2002

Data assimilation is an approach to studying geodynamic models consistent simultaneously with observables and the governing equations of mantle flow. Such an approach is essential in mantle circulation models, where we seek to constrain an unknown initial condition some time in the past, and thus cannot hope to use first-principles convection calculations to infer the flow history of the mantle. One of the most important observables for mantle-flow history comes from models of Mesozoic and Cenozoic plate motion that provide constraints not only on the surface velocity of the mantle but also on the evolution of internal mantle-buoyancy forces due to subducted oceanic slabs. Here we present five mantle circulation models with an assimilated plate-motion history spanning the past 120 Myr, a time period for which reliable plate-motion reconstructions are available. All models agree well with upper- and mid-mantle heterogeneity imaged by seismic tomography. A simple standard model of whole-mantle convection, including a factor 40 viscosity increase from the upper to the lower mantle and predominantly internal heat generation, reveals downwellings related to Farallon and Tethys subduction. Adding 35% bottom heating from the core has the predictable effect of producing prominent high-temperature anomalies and a strong thermal boundary layer at the base of the mantle. Significantly delaying mantle flow through the transition zone either by modelling the dynamic effects of an endothermic phase reaction or by including a steep, factor 100, viscosity rise from the upper to the lower mantle results in substantial transition-zone heterogeneity, enhanced by the effects of trench migration implicit in the assimilated plate-motion history. An expected result is the failure to account for heterogeneity structure in the deepest mantle below 1500 km, which is influenced by Jurassic plate motions and thus cannot be modelled from sequential assimilation of plate motion histories limited in age to the Cretaceous. This result implies that sequential assimilation of past plate-motion models is ineffective in studying the temporal evolution of core–mantle-boundary heterogeneity, and that a method for extrapolating present-day information backwards in time is required. For short time periods (of the order

One contribution of 14 to a Discussion Meeting 'Chemical reservoirs and convection in the Earth's mantle'.

of perhaps a few tens of Myr) such a method exists in the form of crude 'backward' convection calculations. For longer time periods (of the order of a mantle overturn), a rigorous approach to extrapolating information back in time exists in the form of iterative nonlinear optimization methods that carry assimilated information into the past through the use of an adjoint mantle convection model.

Keywords: mantle convection; Earth's interior; geodynamics; data assimilation

1. Introduction

Since the advent of global seismic tomography more than two decades ago (Dziewonski *et al*. 1977) seismic-imaging studies have provided powerful constraints on mantle flow. Starting with the pioneering studies of Masters *et al*. (1982), Dziewonski (1984) and Hager & Clayton (1989), seismologists have demonstrated that the Earth's mantle is heterogeneous on the largest scales, with a prominent pattern of fast lower-mantle seismic-velocity anomalies concentrated into a ring-like structure that circumscribes the Pacific. Richards & Engebretson (1992) showed that this pattern correlates with the Earth's relatively recent Cenozoic and Mesozoic subduction history, i.e. with the location of cold mantle downwellings at convergent plate boundaries over the past 200 Myr. Their findings illustrated the relationship between deep-mantle structure and the history of plate motion, and supported the view that tomographic images are 'snapshots' of a convecting mantle. The seismic studies have matured to the point where the largest features are becoming well resolved throughout the mantle, and the long-wavelength mantle heterogeneity structure is now widely agreed upon (Masters *et al*. 1996; Li & Romanowicz 1996; Ritsema & van Heijst 2000).

In a complementary development, finer spatial scales of mantle heterogeneity have come into our focus with the recent high-resolution seismic-imaging studies of Grand *et al*. (1997) and van der Hilst *et al*. (1997). In fact, considerable attention has been devoted to mapping the fate of oceanic plates subducted since the Cretaceous. As a result, detailed images of the Farallon slab under North America (van der Lee & Nolet 1997) and the numerous slabs in the western Pacific (van der Hilst 1995) are now available. Attention has also turned to the Mesozoic slabs of Jurassic age, buried in the Asian mantle under Siberia. These ancient slabs were left behind from the closure of the Mongol-Okhotsk Ocean (van der Voo *et al*. 1999). The consensus emerging from the seismic studies is consistent with highly time-dependent flow, where some slabs enter the lower mantle relatively unimpeded, while others interact with the transition zone (van der Hilst 1995).

While seismologists progressed in mapping mantle heterogeneity, geodynamicists advanced in mapping the parameter space of three dimensional (3D) spherical mantle convection (Baumgardner 1985; Glatzmaier 1988; Bercovici *et al*. 1989). Owing largely to the dramatic increase in computational power of modern parallel computers, convection models are now available with sufficient spatial resolution to approximate the dynamic regime of global mantle flow (Tackley *et al*. 1993; Bunge *et al*. 1996; Zhong *et al*. 2000). Early on, these models emphasized the general character of mantle convection, which involves a number of complicated physical effects. The models highlighted the effects of phase transitions (Tackley *et al*. 1994), heating mode and radial viscosity variations on mantle convection, with some calculations run at Rayleigh numbers as high as 10^8 (Bunge *et al.* 1997). In a series of recent technical breakthroughs, geodynamicists have also begun to simulate some of the most complicated aspects of mantle convection involving the effects of brittle failure along plate margins. They achieved this technical advance either through modelling a mobile weak zone along plate margins (Zhong & Gurnis 1996) or by using relatively complicated laws of strain-weakening rheology (Bercovici 1998). As a result, the generation of plate tectonics can now be studied self-consistently in some mantle convection models (Trompert & Hansen 1998; Tackley 2000; Zhong *et al.* 2000; Richards *et al.* 2001).

Unfortunately, the striking progress of simulating complicated mantle convection processes on a computer is beginning to reveal a fundamental problem of *ab initio* geodynamic simulations. The problem arises because mantle convection is highly sensitive to initial conditions. The initial condition for mantle convection some time in the past is of course unknown. This lack of initial-condition information is of great concern. It implies that mantle convection calculations cannot be used to model the flow structures mapped by seismologists. Simply put, we cannot hope to explain present-day mantle heterogeneity by running a mantle convection model forward in time from some well-defined initial state, even if we had a perfect mantle convection model, because such a well-defined initial state is, of course, unknown. This strong sensitivity to initial conditions ultimately dictates that a predictive mantle convection model capable of reproducing seismic mantle heterogeneity is, in a sense, inescapably doomed to failure.

Hager & O'Connell (1979) showed the initial-condition problem can be at least partly overcome through *data assimilation*. By including, i.e. assimilating, present-day plate motion into analytic flow calculations, Hager & O'Connell (1979) computed global mantle flow consistent with their model and the assimilated data. Ricard *et al.* (1993) went one step further with the assimilation problem. Using a history of subduction, they estimated the Mesozoic and Cenozoic evolution of mantle-buoyancy forces and included these buoyancy forces into global mantle flow, thus pioneering data assimilation in time-dependent geodynamic models. Stated in simple terms, the purpose of data assimilation in mantle convection is as follows: using all available information, determine as accurately as possible the state of mantle flow at any given time. The available information consists first of the observations proper, plate motions in the case of Hager & O'Connell (1979) and Ricard *et al.* (1993). The second source of information is the dynamic model, and more precisely the physical laws governing the flow. These physical laws are fundamentally the principles of conservation of mass, momentum and energy, and a computational model is nothing other than a numerically usable statement of these principles. Before we come to the technical aspects, we recall that the initial-condition problem is encountered in many areas of geophysical flow. Not surprisingly, data assimilation is used to overcome it. Numerical weather-prediction models, for example, use a range of data assimilation techniques (Talagrand 1997). The approach is also emerging prominently in oceanography (Bennett 1992; Wunsch 1996). Most often, data are assimilated into a computational model through a process known as 'sequential filtering' (Wunsch 1996). Here the model is integrated over the time period for which observations have been made. Whenever the model reaches an instant where observations are available, the model is 'updated' or 'corrected' with the new observation. The calculation is then restarted from the updated state and the process repeated until all available information has been used.

Bunge *et al.* (1998) used this approach to compute mantle circulation models (MCMs). Starting from an assumed initial condition for the Late Cretaceous mantle (necessarily an approximation for 'true' Cretaceous mantle heterogeneity, which is of course unknown) they assimilated a history of Mesozoic and Cenozoic plate motion compiled by Lithgow-Bertelloni & Richards (1998) into 3D spherical mantle convection. The assimilation updated the surface velocities computed from their high-resolution mantle convection simulation with the record of past plate motion and spanned the past 120 Myr, a time period for which reliable plate reconstructions are available. Bunge *et al.* (1998) studied a simple mantle convection model of uniform chemical composition, heated primarily from within by radioactivity with a modest 20% component of bottom heating. The model also included a significant radial viscosity increase by a factor of 40 in the lower mantle and the lithosphere relative to the asthenosphere, as well as the dynamic effects of two well-established mantle phase transitions at depths of 410 and 670 km.

In this paper, we extend these models to explore a larger range of modelling parameters and to probe the effects of realistic variations in the heating mode, the radial mantle-viscosity profile and the strength of the two phase transitions, all of which are known to affect vigorous 3D spherical mantle convection (Tackley *et al.* 1994; Bunge *et al.* 1997). Our calculations define a range of simple whole-mantle convection models, consistent with the governing equations of mantle flow, tectonic constraints provided by past plate-motion models and seismic tomographic observations of the large-scale mantle-heterogeneity structure. In the following sections, we briefly describe our numerical solution strategy and define the modelling parameters and thermodynamic reference state of our simulations. We then present the lateral and spectral heterogeneity content of five MCMs, all of which assimilate a plate-tectonic history inferred by Lithgow-Bertelloni & Richards (1998) for Mesozoic and Cenozoic global plate motion. We compare the MCMs with the high-resolution shear body wave study of Grand *et al.* (1997). Successful models allow for mass exchange between the upper and the lower mantle, account for a depthwise increase in mantle viscosity and include a substantial amount of bottom heating from the core. In fact, the models presented here agree remarkably well with the general character of mantle heterogeneity inferred from seismic tomography, both in their overall spectral heterogeneity content and in their particular location of cold downwelling slabs in the upper and mid-mantle.

We discuss the potential of using MCMs with assimilated plate-motion histories to construct time-dependent mantle flow models. Applications of these models include testing competing plate-tectonic hypotheses with seismic tomography to explore the consistency between tectonic reconstructions of past plate motion and seismic images of subducted slabs. Applications also include the potential to extract synthetic seismic datasets from the geodynamic models to compare these models more directly with seismic observables. Finally, we address the most serious shortcoming in all current MCMs with assimilated plate-motion histories. The limitation arises because well-constrained plate reconstructions are restricted to the past 120 Myr, a time period almost certainly less than the time-scale for generating thermal heterogeneity in the mantle. The problem is aggravated by the fact that geodynamicists assimilate past plate-motion histories into their models through sequential filtering. The approach carries information forward in time, from the past into the present. But no information is carried back in time from the present to improve our estimates of mantle flow at some earlier time using observations made later on. The result is profound: geodynamicists cannot reliably infer the heterogeneity structure of the deepest mantle, leaving our estimates of the deep-mantle heterogeneity sensitive to the assumed initial condition. Arguably, this constraint precludes us from overcoming the initial-condition problem with sequentially assimilated plate histories: a difficulty that is, in fact, evident from the Jurassic slabs buried under Siberia, as it is indeed not obvious how plate-motion histories that are limited in age to the Cretaceous can be applied to modelling mantle heterogeneity associated with subduction in the Jurassic.

We conclude by noting that the initial-condition problem is not necessarily insurmountable. A more powerful approach to data assimilation involves global smoothing (Bennett 1992; Wunsch 1996), which explicitly carries information back in time from the present. The approach is thus well suited for data assimilation in geodynamic models, where information on present-day mantle structure is infinitely more detailed than our knowledge of the mantle at some earlier time. Arguably, the most important information on mantle structure comes from seismic-imaging studies. It would therefore seem advantageous to attempt to assimilate seismic data into time-dependent mantle circulation models. This can be done with an *adjoint* MCM, which allows us to smooth constraints from the assimilated seismic data globally over the entire time-domain of the MCM by relating present-day mantle structure explicitly to flow at some earlier time. The adjoint equations for mantle convection have been derived recently together with simple numerical modelling experiments to demonstrate that mantle flow can in principle be inferred back in time for 100 Myr (Bunge *et al.* 2002). We suggest that data assimilation using adjoint MCMs holds some promise for overcoming the initial-condition problem in mantle flow.

2. Fluid mechanics of mantle convection

We solve the mantle convection equations using the numerical modelling code TERRA (Bunge & Baumgardner 1995). TERRA solves for the momentum and energy balance of mantle convection at infinite Prandtl number (no inertial forces) in a spherical shell with the inner radius being that of the outer core and the outer radius corresponding to the Earth's surface. In all the following calculations we use a numerical mesh with more than 10 million finite elements, allowing us to provide a grid-point resolution of *ca.* 50 km throughout the mantle. With this resolution, we are able to resolve a characteristic thermal boundary thickness of the order of 200 km.

We incorporate the dynamic effects of mantle compressibility through the anelastic liquid approximation (Glatzmaier 1988) using a Murnaghan equation (Murnaghan 1951). The reference state is identical to that of Bunge *et al.* (1997). Heat capacity and thermal conductivity are held constant, with the former being set to $1.134 \times 10^3\ \mathrm{J\,kg^{-1}\,K^{-1}}$ and the latter to $6.0\ \mathrm{W\,m^{-1}\,K^{-1}}$. An internal heating rate of $6.0 \times 10^{-12}\ \mathrm{W\,kg^{-1}}$ is imposed, roughly the chondritic value (Urey 1956). We choose an upper-mantle viscosity of 8.0×10^{21} Pa s. The value is somewhat larger than estimates of Earth's upper-mantle viscosity derived from studies of post-glacial rebound (e.g. Mitrovica 1996), due to computational limitations. A substantial viscosity increase from the upper to the lower mantle is included, as suggested by studies of the geoid

Table 1. *Parameter values used in this study*

parameter	value
outer shell radius	6370 km
inner shell radius	3480 km
T_{surface}	300 K
T_{CMB} (for internally heated cases)	1900 K
T_{CMB} (for bottom-heated case with high viscosity)	3300 K/ 3500 K
η, upper mantle	8.0×10^{21} Pa s
η, lower mantle	40η upper mantle
η, lithosphere	100η upper mantle
thermal conductivity k	6.0 W m^{-1} K^{-1}
internal heating rate Q_{int}	6.000×10^{-12} W kg^{-1}
heat capacity	1.134×10^{3} J kg^{-1} K^{-1}
Ra_{H} (based on η upper mantle)	1.0×10^{8}
phase-change parameters	
γ_{410}	2 MPa K^{-1}
$\rho_{410}/\triangle\rho_{410}$	3918 kg m^{-3}/230 kg m^{-3}
α_{410}	3.026×10^{-5} K^{-1}
P	0.034
γ_{670}	-3 MPa K^{-1}
$\rho_{670}/\triangle\rho_{670}$	4117 kg m^{-3}/380 kg m^{-3}
α_{670}	2.671×10^{-5} K^{-1}
P	-0.087

(Ricard *et al.* 1993) and post-glacial rebound (Mitrovica 1996). In all calculations that follow, mantle viscosity increases monotonically through the transition zone by a factor of 40 (unless specified otherwise), while the viscosity of the lithosphere—the upper 100 km in our models—is always larger by factor of 100 relative to the upper mantle. The thermal boundary conditions are always constant temperature at the surface and the core–mantle boundary (CMB), with the CMB temperature specified to result in a bottom heat flux of less than 1% of the global surface heat flux in our models with predominantly internal heat production. We also investigate two models with a substantial heat flux from the core (35% of the total surface value). In these models we increase the CMB temperature to accommodate the larger bottom heat flux. Mechanical boundary conditions are specified (plate) velocities at the surface and free-slip (no shear-stress) at the CMB. The parameter values of our calculations are listed in table 1. With these modelling parameters, the intensity of internally heated convection in our models is characterized by a Rayleigh number, Ra_H, of 10^8, based on the upper-mantle viscosity.

Arguably the most important modelling assumption in our data-assimilation models is that of the initial condition. We adopt the following simplifying choice: we approximate the unknown Mid-Cretaceous mantle heterogeneity as a quasi-steady

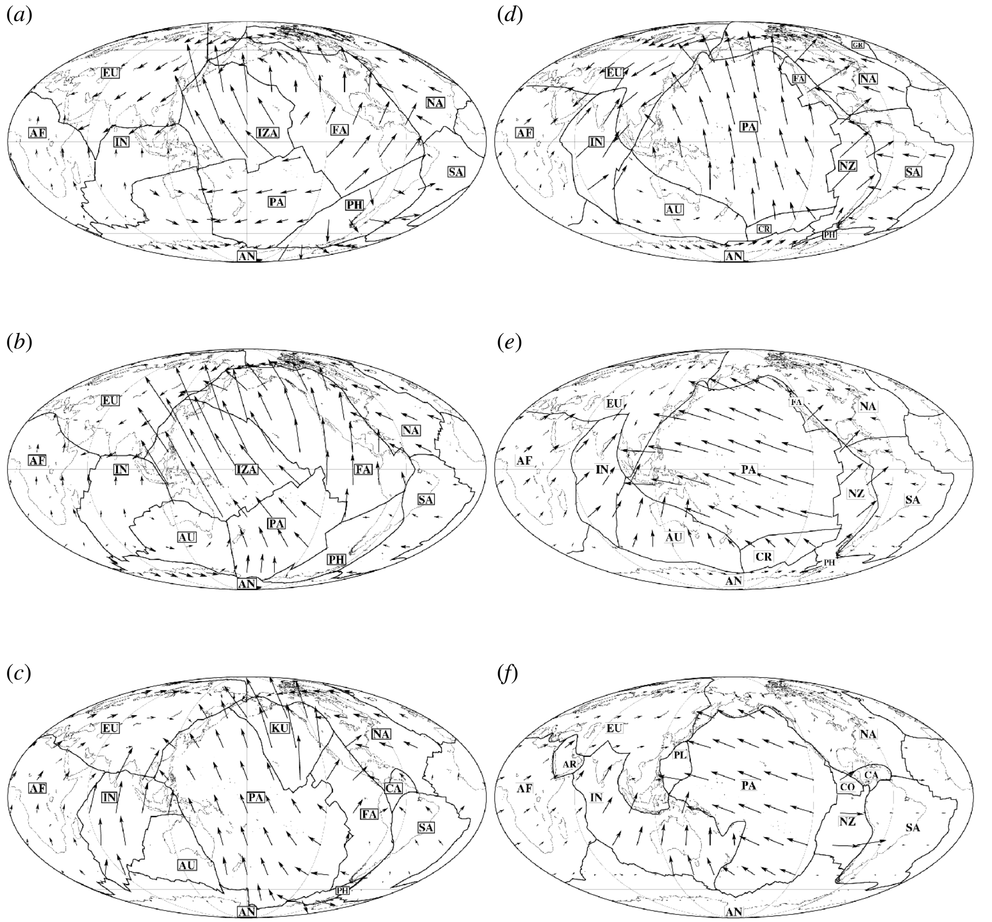

Figure 1. Plate boundary maps for Mesozoic and Cenozoic plate stages (*a*) 119–100 Ma; (*b*) 94–84 Ma; (*c*) 74–74 Ma; (*d*) 48–43 Ma; (*e*) 43–25 Ma and (*f*) present day (10–0 Ma) (from Lithgow-Bertelloni & Richards 1998) with Cenozoic plate motion compiled from the global reconstructions of Gordon & Jurdy (1986). Arrows indicate the direction of plate motion. Their length is proportional to the plate speed. AF denotes Africa; AN, Antarctica; AR, Arabia; AU, Australia; CA, Caribbean; CO, Cocos; CR, Chatham Rise; EU, Eurasia; FA, Farallon; IN, India; KU, Kula; NA, North America; NZ, Nazca; PA, Pacific; PL, Philippines; PH, Phoenix; and SA, South America. In the Mesozoic the ancient Izanagi (IZA), Farallon (FA), Kula (KU) and Phoenix (PH) plates occupy most of the Pacific Basin. Today these plates have largely disappeared. In the Cenozoic, the Pacific (PA) plate is inferred to undergo a rapid change from predominantly northward to westward motion after *ca.* 43 Myr.

state of mantle flow with the oldest available plate reconstruction corresponding to Mid-Cretaceous plate motion (119 Ma, see figure 1), and assimilate Mid-Cretaceous plate motion for all of the Earth's history (4.5 Gyr) prior to that time. We account for the reduced convective vigour of our models by scaling the root-mean-square (RMS) plate velocities so that convective motion is neither increased nor reduced by the assimilated velocities, i.e. we scale the RMS plate velocity to match the RMS surface velocity of convection with no imposed plate motion, thus keeping the model Péclet number unchanged. The smaller surface velocities of our calculations imply a slower overall temporal evolution of our models compared with the Earth. Consequently, absolute times are not meaningful in our models. Instead we express time in terms of transit times (Gurnis & Davies 1986*a*), where we define one transit time as the ratio of mantle depth to model RMS surface velocity. In all calculations that follow, model time is normalized to 'Earth time' by multiplying by the ratio of Earth's plate RMS velocities (*ca.* 5 $\mathrm{cm\,yr^{-1}}$) to the RMS surface velocity of convection with no imposed plate motion (*ca.* 1.5 $\mathrm{cm\,yr^{-1}}$). Thus imposing Mid-Cretaceous plate motion for 4.5 billion years of 'Earth time' corresponds to a model time of *ca.* 13.5 billion years. Mantle flow after 4.5 billion 'Earth years' of assimilated Mid-Cretaceous plate motion represents heterogeneity in quasi steady state with the imposed plate motion, and in lieu of other information we may regard it as a crude approximation for large-scale thermal heterogeneity in the Mid-Cretaceous mantle.

3. Comparison of fluid and seismic mantle models

(*a*) *Lateral heterogeneity*

Before proceeding, we note a key result from our previous work on MCMs. In Bunge *et al.* (1998) we performed simple model experiments designed to demonstrate the effective spin-up time-scale associated with changes in plate motions. We probed this question by first running convection models for a long time up to quasi-equilibrium with a single regime of imposed plate motions (the 119–100 Ma stage) and then suddenly imposing present-day plate motions. The models thus involved only two plate-motion stages and showed that (depending on the exact model parameters used) the approximate re-equilibration time for the adjustment of mantle convection to the new regime of plate motions varied from *ca.* 50 Myr for the upper and mid-mantle to *ca.* 150–200 Myr for the deep mantle. These fundamental response times (applicable, of course, only to whole-MCMs) are important to keep in mind as we consider the effects of changing plate motions in MCMs constrained by plate-motion histories. For example, they imply directly that assimilation of plate-motion data into mantle flow through sequential filtering cannot be used to infer even the recent evolution of CMB structure, because well-constrained plate motions are simply not available for a long enough period of time (Richards *et al.* 2000).

With the above caveat in mind, we now turn our attention to study the lateral heterogeneity of MCMs with assimilated plate-motion histories. Our reference model is decidedly simple. It includes pure internal heat generation and a viscosity increase of a factor of 40 from the upper to the lower mantle in what may be regarded roughly as a geodynamic 'standard model' for whole-mantle flow (Davies & Richards 1992). The initial condition for our calculation is mantle flow in quasi-steady state with Mid-Cretaceous plate motions (119 Ma), as described above. Starting from this initial condition we integrate convection forward in time for 100 Myr of Earth time and assimilate past plate motions deduced from the global reconstructions of Lithgow-Bertelloni & Richards (1998) (see figure 1) as a time-dependent surface-velocity boundary condition. RMS plate velocities are scaled to match the surface RMS velocities of convection without assimilated plate motion, as noted above. Figure 2*b* shows the lateral heterogeneity of our data-assimilation model in the transition zone (at a depth of 670 km). We also present a tomographic model of mantle heterogeneity (figure 2*a*) inferred from the shear body-wave study of

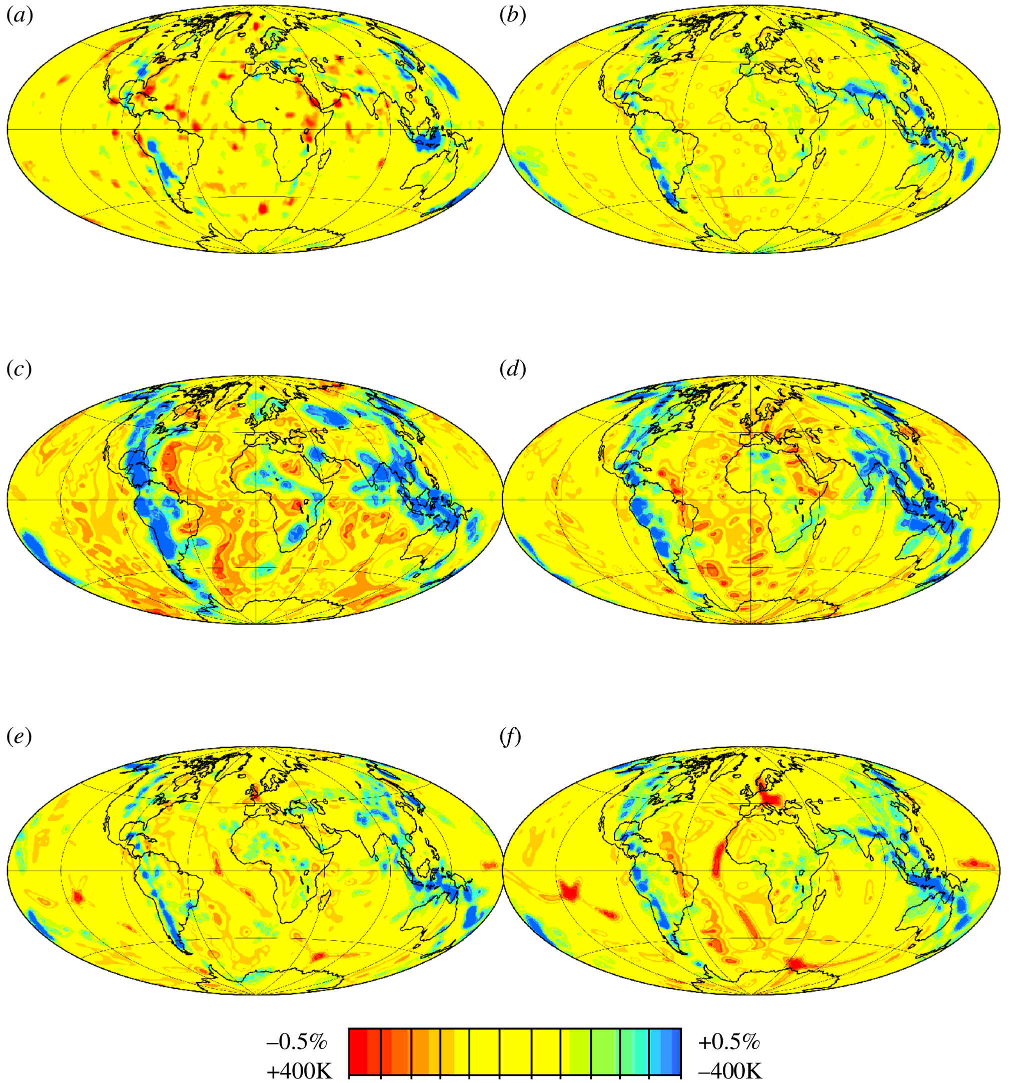

Figure 2. Demeaned lateral heterogeneity maps at a depth of 670 km for Grand *et al.*'s S-wave model (a) and the five MCMs discussed in the text. (b) Reference MCM with pure internal heat generation and a factor-40 viscosity increase in the lower mantle. (c), (d) Same as (b) but with (c) the effects of two mantle phase reactions or (d) a viscosity contrast of factor 100 between the upper and the lower mantle. (e), (f) Same as (b) and (d) but with 35% added core heating. In the MCMs, blue denotes cold and red denotes hot (measured on a scale of ±400 K). For the seismic model, blue is fast and red is slow (measured on a scale of $\pm0.5\%$). The seismic study shows slabs associated with subduction under the Americas, India and the western Pacific. The reference MCM, part (b), is similar. Parts (c) and (d) show strong transition-zone heterogeneity due to slabs delayed on their way into the deep mantle. Parts (e) and (f) show additional high-temperature anomalies due to hot rising mantle flow.

Grand *et al.* (1997). The secondary-wave (S-wave) model is remarkably similar to the independent compressional primary-body-wave tomographic model of van der Hilst *et al.* (1997). Looking first at the tomographic model, figure 2*a* shows sheets of fast seismic-velocity anomalies associated with subducted slabs beneath North and South America and corresponding to the Farallon and Nazca plates. There are also fast seismic-velocity anomalies under India and the western Pacific associated with Cenozoic subduction of the Indian and Pacific plates beneath Eurasia. Isolated point-like low-velocity anomalies exist, for example, under the Red Sea Rift and the East African Rift. The overall heterogeneity of the data-assimilation model (figure 2*b*) is characterized by a similar pattern, with cold anomalies concentrated under places of past plate convergence, although there is a lack of hot active mantle upwellings, owing to the absence of core heating. Away from mantle downwellings, temperatures are nearly uniform, as expected for internally heated convection.

We proceed in figure 2*c* by adding the dynamic effects of the 410 km and 670 km phase transitions to our reference model, while leaving all other modelling parameters unchanged. We use a Clapeyron slope of $\gamma_{410} = 2\ \mathrm{MPa\,K^{-1}}$ to model the 410 km olivine-to-spinel phase transformation and a value of $\gamma_{670} = -3\ \mathrm{MPa\,K^{-1}}$ for the β-spinel-to-perovskite transition at a depth of 670 km, in agreement with experimental data (e.g. Katsura & Ito 1989; Akaogi & Ito 1993). Our choices for γ_{410} and γ_{670} imply values of the dynamically significant phase-change buoyancy parameter (Christensen & Yuen 1984) of $P_{410} = 0.034$ and $P_{670} = -0.087$, respectively (see table 1). The inhibiting buoyancy effects of the 670 km phase reaction cause upwellings and downwellings to pause in the transition zone, as expected. There are also some downwellings away from plate boundaries under slow moving plates, such as Africa, arising from thermal boundary-layer instabilities. The delay of mantle flow through the transition zone increases the overall amplitude of transition-zone heterogeneity compared with the standard model (figure 2*b*), in agreement with earlier mantle convection studies (Solheim & Peltier 1994; Tackley *et al.* 1994; Bunge *et al.* 1997). But there is little effect otherwise. The sensitivity of mantle circulation to increases in the radial mantle-viscosity profile is probed by examining convection involving a steep, factor 100, viscosity jump from the upper to the lower mantle (figure 2*d*). All other modelling parameters of the high-viscosity case are held unchanged from the standard model in figure 2*b*. As expected, there is sluggish mass transport from the upper to the lower mantle, not unlike the reduced mass transport we observe in mantle flow involving the effects of the endothermic phase reaction. As a result, downwellings are delayed, with numerous slabs concentrated at the upper/lower-mantle boundary. The sluggish flow of slabs into the deeper mantle is particularly evident in regions with substantial Cenozoic subduction. An example is the mantle beneath the western Pacific, where subduction rates increased dramatically after the Pacific plate-motion change from a predominantly northward to a more westward motion some 43 Ma (see figure 1). Not surprisingly, we find numerous Cenozoic slabs in this region, a heterogeneity pattern that may be compared with the S-wave study of Grand *et al.* (1997). We complement our internally heated convection models with two calculations that involve substantial heating from the core, to explore the sensitivity of mantle flow to bottom heating. Adding 35% core heat flux either to the standard model (figure 2*b*) or to the high-viscosity case (figure 2*d*) results in the mantle heterogeneity shown in figure 2*e*, *f*. The modelled core heat flux is substantially larger than that which has been estimated for the mantle based on observations of the dynamic topography over hotspots (e.g. Sleep 1990). The core-heated model in figure 2*e* shows additional hot upwellings located under the Pacific and the Atlantic. Otherwise, the general heterogeneity character with cold mantle downwellings concentrated under plate-convergence zones is similar to our internally heated convection cases. The hot anomalies are more pronounced in the high-viscosity model with 35% bottom heating (figure 2*f*). An intensification of the anomalies in this model is expected because upwellings require larger thermal buoyancy while passing through the stiffer lower mantle compared with the model in figure 2*e*.

We next examine the mid-mantle heterogeneity at a depth of 1500 km (figure 3) in our models. At this depth the S-wave study (figure 3*a*) is dominated by a prominent fast seismic-velocity anomaly located under eastern North America, the Caribbean and the northernmost part of South America due to Farallon subduction. Another fast anomaly follows the Alpine–Himalayan mountain belt and reflects subduction associated with the closure of the ancient Tethys Ocean. There are also two pronounced low-velocity anomalies under Africa and the Azores. Heterogeneity in the standard model (figure 3*b*) is similar, with slabs buried under North and South America and under the Alpine–Himalayan suture, although there is a lack of hot thermal anomalies as noted earlier, due to the absence of core heating. A similar heterogeneity character is evident from the phase-change-modulated case in figure 3*c* and the model in figure 3*d* with a high-viscosity lower mantle. The major difference between both models and the reference case is due to the slower overall sinking velocities of subducted slabs. As a result, mid-mantle heterogeneity is dominated by downwellings corresponding to earlier stages of the assimilated plate-motion history. The bottom-heated cases in figure 3*e*, *f* include substantial hot upwelling flow anomalies in addition to the downwelling slabs that characterize all MCMs. These upwellings are concentrated into broadly similar regions in the mid-Atlantic and the eastern Pacific with thermal anomalies comparable with the thermal perturbations associated with subducted slabs: an observation that agrees well with the S-wave study, where the prominent low-seismic-velocity anomaly under Africa is comparable with seismic heterogeneity associated with subducted slabs. The most substantial difference is the location of the MCM upwellings relative to the slow seismic anomalies in Grand *et al.*'s (1997) model, which is particularly striking for the slow seismic feature under Africa. Our bottom-heated MCMs show hot upwellings, not under Africa, but located several thousand kilometres further west, beneath the mid-Atlantic.

CMB heterogeneity in our MCMs is investigated in figure 4. Here the bottom-heated models (figure 4*e*, *f*) are characterized by strong lateral heterogeneity variations associated with a thermal boundary layer. The spatial heterogeneity pattern agrees remarkably well between the two bottom-heated models. However, as noted earlier in the mid-mantle panels in figure 3, there is a substantial difference in the location of the hot thermal anomalies relative to the S-wave study, especially for the pronounced low-seismic-velocity anomaly under Africa. The great similarity of the bottom-heated cases is striking, given that both models show small but noticeable differences in upper and mid-mantle flow at depths of 670 and 1500 km. We return to the internally heated MCMs (figure 4*b*–*d*) and verify a broadly similar spatial pattern of warm and cold temperature anomalies, while noting that overall heterogene-

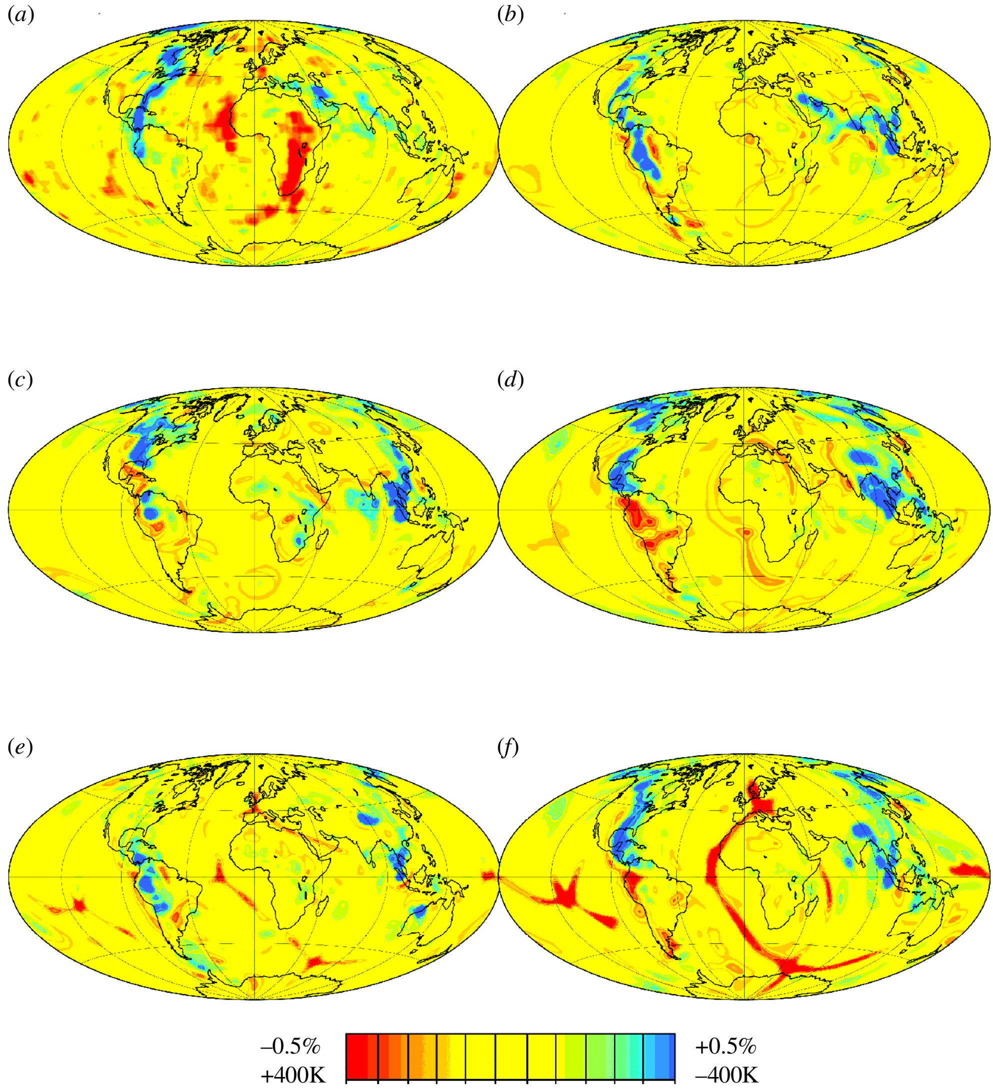

Figure 3. Same maps as figure 2, but for the mid-mantle at a depth of 1500 km. Grand *et al.*'s seismic study, (*a*), is dominated by fast seismic anomalies under the Americas and India arising from Farallon and Tethys subduction. There is also a prominent low-seismic-velocity anomaly under Africa. The reference MCM, part (*b*), is similar, but lacking hot thermal anomalies due to the absence of core heating. Parts (*c*) and (*d*) show thermal anomalies associated with subduction, but with slabs corresponding to earlier tectonic regimes, due to the delayed flux of slabs into the lower mantle. Part (*c*) shows the effects of two mantle phase reactions, and (*d*) shows the effects with a viscosity contrast factor of 100 between the upper and the lower mantle as in figure 2. Parts (*e*) and (*f*) (35% added core heating) show high-temperature anomalies associated with hot rising mantle flow. Note that all MCMs place the Farallon slab *ca.* 1500 km further west of its location in Grand *et al.*'s model, which probably reflects the fact that we do not explicitly account for low-angle subduction under North America during the Late Cretaceous/Eocene Laramide orogeny.

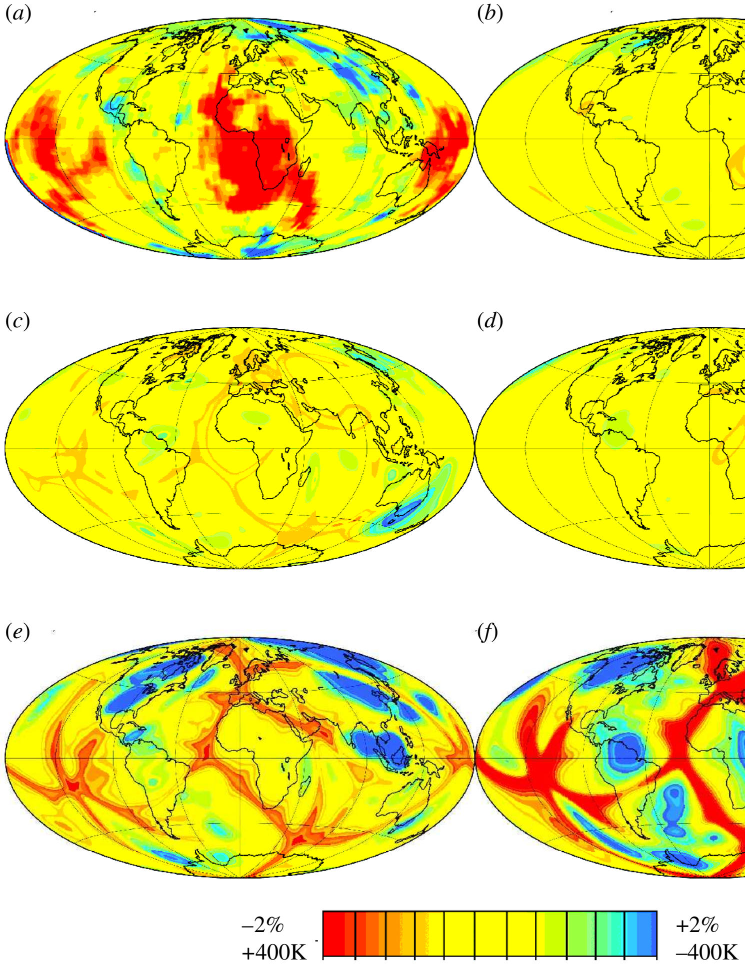

Figure 4. Same maps as figure 3, but for the CMB at a depth of 2800 km. The seismic study by Grand *et al.* (1997), (a), is plotted on a scale of $\pm 2.0\%$ and dominated by a dramatic low-seismic-velocity anomaly under Africa and the Pacific with seismically faster mantle in the intervening regions. The increase in heterogeneity amplitude by a factor of four relative to the upper and mid-mantle is probably due to chemical heterogeneity at the mantle base. All internally heated MCMs (b), (c) and (d) are characterized by the near absence of thermal heterogeneity owing to the absence of heating from the core. The bottom-heated models (e) and (f) show a near identical thermal heterogeneity pattern that correlates with the oldest assimilated plate-motion stage of 119–100 Ma (figure 1) due to the artificial nature of the assumed initial condition (see text).

ity amplitudes are markedly subdued. The small heterogeneity amplitude contrasts sharply with the strong thermal heterogeneity observed in the bottom-heated models and differs from the pronounced CMB heterogeneity amplitudes inferred from Grand *et al.*'s S-wave study. Weak thermal heterogeneity is, of course, expected in our internally heated cases, owing to the absence of a lower thermal boundary layer at the bottom of the mantle.

(*b*) *Spectral heterogeneity*

A useful way to compare geodynamic and seismic Earth models is through spectral heterogeneity maps (SHMs), at least in a stochastic sense. These maps contour the spectral RMS amplitude as a function of mantle depth and spherical harmonic degree (Tackley *et al.* 1994). Figure 5*b* shows the SHM for our standard model. Heterogeneity is dominated by large-scale structure concentrated at low harmonic degrees, as expected for convection involving the effects of plate motion and viscosity stratification (Bunge & Richards 1996). We note that, even without bottom heating, the strongest heterogeneity occurs at degree 2 near the bottom of the mantle. Adding the two mantle phase transitions (figure 5*c*) or a high-viscosity lower mantle (figure 5*d*) adds an intermediate-wavelength heterogeneity near a depth of 670 km with little effect otherwise. Adding 35% core heating has the effect of dramatically strengthening the amplitude of heterogeneity in the lower thermal boundary layer in our bottom-heated cases (figure 5*e*, *f*). These characteristics may be compared with Grand *et al.*'s model (figure 5*a*), where strong heterogeneity amplitude at the lowest spherical harmonic degrees 2–4 is concentrated near the Earth's surface and the bottom of the mantle.

In fact, comparison of the SHM for Grand *et al.*'s model with any of the MCMs shown in figure 5 reveals that, overall, the MCMs do not mimic the relative levels of heterogeneity found in seismic tomography. At the same time, the actual shape of mid-mantle heterogeneity is rather well-modelled, as seen in figures 2–4. The explanation for the failure of MCMs to account for the strong concentration of heterogeneity amplitude near to the top and bottom of the mantle is clear: Grand *et al.*'s model, like all global tomography models, is dominated in terms of heterogeneity amplitude by the uppermost and lowermost mantle signatures, both of which are probably due to chemical boundary-layer heterogeneities not modelled in our MCM approach. The lithospheric signal (uppermost 300 km or so) strongly reflects the presence of deep continental roots ('tectosphere'), which in turn are thought to reflect long-lived chemical heterogeneity carried beneath ancient continental areas (see, for example, Jordan 1978). The lowermost mantle seismic-velocity anomalies are likewise believed to reflect chemical heterogeneity, as evidenced by the negative correlation between bulk-sound and shear-wave speeds in this region (e.g. Kennett *et al.* 1998). In other words, whole-mantle MCMs may stand a chance of predicting thermal structure in the mantle interior, but are inherently incapable of predicting the seismic signatures of the lithosphere and CMB region. The larger CMB heterogeneity amplitude modelled from our MCMs with strong core heating goes some way towards explaining the CMB signature observed in Grand *et al.*'s model. But it would be premature to conclude that the strong heterogeneity amplitude of the CMB region requires high core heat flux. The SHMs therefore remind us that the development of MCMs from data assimilation or from other techniques is at a stage of infancy, even if the 'fixes' necessary for greater realism are fairly obvious.

4. Discussion

We have studied five MCMs with assimilated plate-motion histories, but we have by no means exhausted the relevant parameter space. For example, we have not investigated the possible range of mantle viscosity profiles and we have not studied the effects of all reasonable variations in phase buoyancy parameters. Our simple MCMs

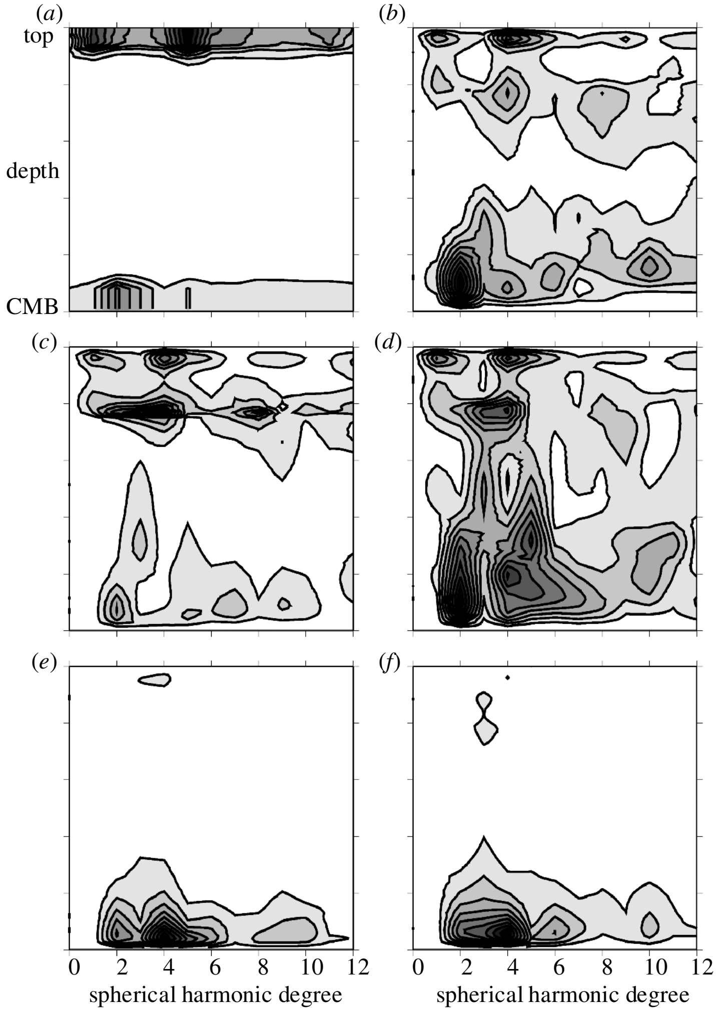

Figure 5. Spectral heterogeneity maps (SHMs) for the five MCMs and the S-wave study of Grand *et al.* (1997) shown in figures 2–4. (*a*) S-wave study. Strong heterogeneity probably associated with chemical variations dominates the top and bottom of the mantle. (*b*) Reference MCM (see text). Heterogeneity is concentrated into the gravest spherical harmonic degrees 2–4 at the top and bottom of the mantle. Parts (*c*) and (*d*) show the same maps as in (*b*), but with (*c*) the effects of two mantle phase reactions, or (*d*) with a viscosity contrast factor of 100 between the upper and the lower mantle. An additional heterogeneity amplitude exists in the transition zone. Parts (*e*), (*f*) show the same maps as in (*b*) and (*d*) but with 35% added core heating. Strong heterogeneity associated with the lower thermal boundary layer dominates the SHMs. RMS spectral amplitude is contoured as a function of mantle depth (surface at the top, CMB at the bottom) and spherical harmonic degree (0–12). Each panel is normalized to the maximum amplitude for that panel, and there are 10 contour intervals.

do not include the effects of lateral viscosity variations arising from lateral variations in temperature and strain rate (e.g. Tackley 2000; Trompert & Hansen 1998; Zhong *et al.* 2000). An even more important omission is that we have not considered the effects of compositional stratification, which are believed to be important in the deep mantle (Kellogg *et al.* 1999). The choice of a reduced convective vigour in our models stems mainly from computational considerations. Each model presented here saturates the largest supercomputer available to us (a LINUX-based Beowulf PC cluster). However, our results are sufficient to infer the general response of mantle circulation with 'Earth-like' viscosity stratification, core heating and phase changes at a Rayleigh number of 10^8 to the effects of assimilated plate-motion histories. The response is, in fact, quite predictable. Heterogeneity is dominated by subducted slabs descending into the mantle at convergent plate boundaries. The dominance of long-wavelength structure in our models agrees well with the prominent large-scale mantle heterogeneity structure imaged by seismologists (Dziewonski 1984) and with the red spectrum of the geoid, which has a strong peak at spherical harmonic degrees 2–3. Our models are similar in this respect to the data-assimilation models of Ricard *et al.* (1993), which yield excellent fits to the observed geoid.

There are, however, fundamental limitations. Arguably the most profound result is our inability to resolve deep-mantle structure. The result is easily anticipated from the prediction that deep-mantle advection velocities scale roughly with the logarithm of the upper/lower-mantle viscosity contrast (Gurnis & Davies 1986*b*). The significant depthwise viscosity increase in the mantle implies an effective transit time of the order of 150–200 Myr, as slabs sink through the mantle: a period considerably longer than the time spanned by models of past plate motion. Thus, we should not hope to infer the heterogeneity structure of the deepest mantle from assimilated plate-motion histories spanning only *ca.* 100 Myr. The difficulty is obvious in our bottom-heated models. In fact, both models show nearly identical flow structure at the CMB, despite their different radial viscosity profile. The difficulty is equally apparent from the near-stationary pattern of hot upwelling mantle flow in these models evidenced, for example, by comparing hot mantle regions at the CMB with the locations of high-temperature anomalies in the mid-Atlantic at a depth of 1500 km. The high-temperature anomalies agree well with patches of hot mantle at the CMB, but show little resemblance to the location of the African low-seismic-velocity anomaly in Grand *et al.*'s S-wave study. We can understand the spatial pattern of deep-mantle heterogeneity in our data-assimilation models to be an artefact of the model initialization. This is evident when we compare it with the 119–100 Ma Mid-Cretaceous plate reconstruction (figure 1) and note that it corresponds closely to the location of spreading and subduction plate margins in the reconstructions of Lithgow-Bertelloni & Richards (1998). In other words, deep-mantle heterogeneity in our data-assimilation models is entirely controlled by the oldest assimilated plate-motion stage used to initialize flow in the Mid-Cretaceous mantle. We could, of course, make other assumptions to approximate Mid-Cretaceous mantle heterogeneity, rather than assuming it can be inferred from flow in a quasi-steady state with Mid-Cretaceous plate motion. But, regardless of whatever we may assume for heterogeneity in the Mid-Cretacous, our results demonstrate clearly that sequential assimilation of plate-motion histories into mantle flow is insufficient to overcome the initial-condition problem.

Our finding has important implications for fledgling studies of the temporal evolution of mantle heterogeneity at the CMB. There are a number of attractive reasons for trying to understand time variations in the large-scale structure of the CMB. For example, recent magnetohydrodynamic simulations of the core indicate that the geodynamo is sensitive to changes in CMB heterogeneity (Glatzmaier *et al.* 1999; Bloxham 2000). Palaeomagnetists have long speculated about possible causes for the Cretaceous Normal Superchron (CNS), a remarkable time period lasting from *ca.* 120 to 85 Ma, when the geodynamo occupied a single magnetic polarity. It appears entirely plausible that the great stability of the geodynamo in the Mid-Cretaceous occurred in response to large-scale temperature variations at the CMB associated with Mesozoic mantle convection. Our results demonstrate that we cannot test this hypothesis in MCMs with sequentially assimilated plate-motion histories (see a more detailed analysis of this problem in Richards *et al.* (2000)).

Our results for heterogeneity in the mid- and upper mantle are more encouraging. Here the MCMs show small but noticeable differences, aside from the first-order observation that cold downwellings agree well with subducted slabs in Grand *et al.*'s S-wave study, implying that plate-motion histories can be used to improve our understanding of flow in the upper and mid-mantle. There is, however, an important additional caveat. When assimilating past plate-motion models, we must realize that tectonic reconstructions, particularly for those plates that have completely disappeared (Izanagi, Phoenix, Kula) or are in the process of disappearing (Farallon), are only approximate, especially the locations of subduction zones and to a lesser extent the poles of rotation. The great uncertainties associated with plate-motion histories imply equally significant uncertainties in the location of mantle downwellings in our models. We take the mid-mantle location of the Farallon plate under North America as an example. All five MCMs show the ancient Farallon slab further west of its location in Grand *et al.*'s seismic study, by *ca.* 1500 km. The displacement is well outside the inherent spatial resolution both in the S-wave study and in our flow calculations, which employ a grid-point resolution of *ca.* 50 km throughout the mantle. It arises probably from an unusual period during the Late Cretaceous/Eocene Laramide orogeny (from 70 to 40 Ma) when the Farallon plate subducted at a shallow angle under North America (Dickenson & Snyder 1978). We can test this plate-tectonic hypothesis explicitly by simulating the effects of low-angle subduction in our models. Assuming a shallow dip angle of the Farallon slab under North America during the Laramide orogeny we find that the MCMs match Grand *et al.*'s image of the Farallon slab rather well (Bunge & Grand 2000). There are numerous other plate-tectonic uncertainties, related especially to the Mesozoic plate boundaries in the western Pacific. For example, the ancient Izanagi subduction zone in the northwestern Pacific is poorly known, implying significant uncertainties in mid-mantle MCM heterogeneity structure under Eurasia. The MCMs thus offer an intriguing mechanism to test competing plate-tectonic hypotheses with tomographic studies to improve past plate-reconstruction models.

The strong local effect of the β-spinel-to-perovskite phase reaction in the transition zone may seem at first surprising. The associated MCM heterogeneity with numerous slabs located at a depth of 670 km is quite unlike the heterogeneity imaged in Grand *et al.*'s S-wave study. The dramatic phase-reaction effect is not easily anticipated, given our modest choice for the value of the Clapeyron slope with $\gamma_{670} = -3\,\mathrm{MPa\,K^{-1}}$. However, there are other factors besides the Clapeyron slope that influence the ability of downwellings to penetrate the lower mantle, such as trench migration, i.e. the lateral movement of subduction zones (Christensen 1996). Considerable trench migration occurred over the past 120 Myr in the Indo–Eurasian plate-convergence zone and the subduction zones surrounding the Pacific, evidenced, for example, by the westward motion of subduction off-shore of North and South America due to the opening of the Atlantic Basin. Trench migration enters our models through the assimilated plate-motion history, although we note that the strong overall effect of the phase reaction would be offset in part if we modelled the enhanced stiffness of cold subducted lithosphere, which promotes slab flow into the lower mantle by acting as a stress guide (Zhong & Gurnis 1994). However, it is clear from our calculations that assimilated plate-motion histories offer important additional constraints on the development of mantle heterogeneity in the transition zone.

We must make another qualifying remark: our bottom-heated models draw 35% of their energy budget from the core, an amount substantially larger than that which has been estimated for the mantle, based on observations of dynamic topography over hotspots (e.g. Sleep 1990). Analog mantle convection experiments indicate that deep-mantle plumes may be captured by large-scale mantle circulation, suggesting that there could be a significant amount of 'hidden' core heat flux in the mantle aside from the heat flux readily associated with plumes (Jellinek *et al.* 2002). In our bottom-heated models we specify a CMB temperature of 3300 K (3500 K for the case with high viscosity, see table 1), arguably a conservative value of that which has been estimated for the core based on the melting temperature of iron (Boehler 2000). Using this thermal boundary condition, the bottom-heated MCMs yield a temperature drop of more than 1000 K across the lower thermal boundary layer, in agreement with independent mineral-physics estimates for the temperature contrast across D'' (Williams 1997). The sharp temperature contrast across the bottom of the mantle is promoted further because the mantle geotherm is likely to be subadiabatic outside of thermal boundary layers (Bunge *et al.* 2001), so a high core heat flux would seem plausible. A significant amount of core heating is suggested by the energy requirements of numerical dynamo models (Glatzmaier & Roberts 1995; Kuang & Bloxham 1997) and would be consistent with thermal history calculations of the core (Buffett *et al.* 1996), although we add that a chemically distinct layer at the mantle base would lower the core heat flux and would help to reduce the excess temperature of mantle plumes (Farnetani 1997) implied by our calculations. The existence of this layer appears likely from geochemical considerations (Hofmann 1997) and has been explored in dynamic models (Kellogg *et al.* 1999).

There is a last remark we must make. Geodynamicists tend to compare their mantle flow models directly with images of mantle heterogeneity derived from tomographic inversions of seismic data. The approach is problematic because the uneven distribution of seismic sources and receivers and the non-uniqueness of the inverse problem impose a complex tomographic filter on mantle structure that should be considered prior to any comparison of geodynamic and seismic mantle models. We could include the effects of tomographic filtering explicitly in our models by computing synthetic travel-time anomalies from the MCMs and inverting these synthetic travel-time residuals for the mantle structure (e.g. Johnson *et al.* 1993). In MCMs, this approach reveals that tomographic filtering is probably minor in areas of high ray density (Bunge & Davies 2001). However, a far more interesting observation can be drawn from such synthetic seismic datasets. The travel-time anomalies obtained from MCMs reveal that the co-location of earthquake sources and mantle downwellings acts to bias the arrival times of the synthetics in a systematic way. The bias is evident from histograms of the synthetic travel-time residuals, which demonstrate that the arrival-time residuals associated with all five MCMs presented here are characterized by a negative mean. In other words synthetic arrival-time residuals in our MCMs reveal that the Earth's seismic velocity structure as sampled by body-waves is fast compared with an average reference Earth as measured, for example, from free oscillations (Davies & Bunge 2001). Extracting synthetic seismic observables from MCMs is an attractive way to advance our understanding of deep Earth structure, especially as seismologists make rapid progress in their abilities to model complex theoretical phenomena of seismic wave propagation (Komatitsch & Tromp 1999; Dahlen *et al.* 2000) and in their efforts to collect new high-resolution datasets on a continental scale (e.g. Meltzer *et al.* 1999).

5. Conclusion

We have studied mantle circulation by sequentially assimilating past plate-motion histories into fluid-dynamic models of Earth's mantle. We observe excellent correlation of cold downwellings in our models, with the location of subducted slabs inferred from seismic images of the mantle. Our calculations define a range of simple whole-MCMs consistent with the governing equations of mantle flow, tectonic constraints from past plate-motion models and seismic tomographic observations of the large-scale-mantle heterogeneity structure. We find that upper- and mid-mantle heterogeneity structure is sensitive to variations in the amount of core heating, the radial mantle viscosity profile, the strength of phase reactions and the uncertainties in the assimilated plate-motion histories, implying that sensitivity studies in MCMs can be applied to improve our estimates of the radial mantle-viscosity profile, the effects of phase reactions, the ratio of internal to external heating and reconstructions of past plate movement.

In contrast, deep-mantle heterogeneity is insensitive to the constraints provided by the available record of Mesozoic and Cenozoic plate motion but is sensitive to the assumed initial condition for heterogeneity in the Mid-Cretaceous mantle. Our results suggest that sequential filtering of plate-motion histories (where the assimilated data influence mantle flow only at later times, but no information is carried back in time from the present) is insufficient to infer the temporal evolution of deep-mantle heterogeneity, which could be modelled from a variational approach to assimilation by incorporating constraints, for example, from seismic data into mantle flow through adjoint MCMs. Over short time periods (perhaps a few tens of Myr) a crude approach to assimilating seismic data into mantle flow can be derived from simple backwards advection of the 'known' present-day state of the mantle (e.g. Steinberger & O'Connell 1997; Bunge & Richards 1992) to study the most recent evolution of CMB structure. However, for longer time-scales, over which thermal diffusion across boundary layers becomes important (*ca.* 50 Myr or more), constraints from seismic tomography must be assimilated into mantle flow through a more powerful approach to assimilation involving adjoint methods, which are clearly superior in recovering the unknown initial conditions of the mantle (Bunge *et al.* 2002). Data assimilation promises to be a rich field for advancing our theoretical understanding of mantle dynamics in the coming decade.

Computations for this work were carried out on a Beowulf cluster at Princeton University's Department of Geosciences and funded by NSF grant EAR-9814635. H.P.B. acknowledges support from NSF grants EAR-0106651 and EAR-9980457.

References

Akaogi, M. & Ito, E. 1993 Refinement of enthalpy measurement of $MgSiO_3$ perovskite and negative pressure–temperature slopes for perovskite-forming reactions. *Geophys. Res. Lett.* **20**, 1839–1842.

Baumgardner, J. R. 1985 Three dimensional treatment of convective flow in the Earth's mantle. *J. Stat. Phys.* **39**, 501–511.

Bennett, A. F. 1992 *Inverse methods in physical oceanography*. Cambridge University Press.

Bercovici, D. 1998 Generation of plate tectonics from lithosphere–mantle flow and void-volatile self-lubrication. *Earth Planet. Sci. Lett.* **154**, 139–151.

Bercovici, D., Schubert, G. & Glatzmaier, G. A. 1989 Three-dimensional spherical models of convection in the Earth's mantle. *Science* **244**, 950–955.

Bloxham, J. 2000 Sensitivity of the geomagnetic axial dipole to thermal core–mantle interactions. *Nature* **405**, 63–65.

Boehler, R. 2000 High-pressure experiments and the phase diagram of lower mantle and core materials. *Rev. Geophys.* **38**, 221–245.

Buffett, B. A., Huppert, H. E., Lister, J. R. & Woods, A. W. 1996 On the thermal evolution of the Earth's core. *J. Geophys. Res.* **101**, 7989–8006.

Bunge, H.-P. & Baumgardner, J. R. 1995 Mantle convection modeling on parallel virtual machines. *Comput. Phys.* **9**, 207–215.

Bunge, H.-P. & Davies, J. H. 2001 Tomographic images of a mantle circulation model. *Geophys. Res. Lett.* **28**, 77–80.

Bunge, H.-P. & Grand, S. P. 2000 Mesozoic plate-motion history below the northeast Pacific Ocean from seismic images of the subducted Farallon slab. *Nature* **405**, 337–340.

Bunge, H.-P. & Richards, M. A. 1992 The backward-problem of plate tectonics and mantle convection (abstract). *Eos* **73**, 281. (Spring Meeting Suppl.)

Bunge, H.-P. & Richards, M. A. 1996 The origin of large scale structure in mantle convection: effects of plate motion and viscosity stratification. *Geophys. Res. Lett.* **23**, 2987–2990.

Bunge, H.-P., Richards, M. A. & Baumgardner, J. R. 1996 Effect of depth-dependent viscosity on the planform of mantle convection. *Nature* **376**, 436–438.

Bunge, H.-P., Richards, M. A. & Baumgardner, J. R. 1997 A sensitivity study of three-dimensional spherical mantle convection at 10^8 Rayleigh number: effects of depth-dependent viscosity, heating mode, and an endothermic phase change. *J. Geophys. Res.* **102**, 11 991–12 007.

Bunge, H.-P., Richards, M. A., Lithgow-Bertelloni, C., Baumgardner, J. R., Grand, S. P. & Romanowicz, B. 1998 Time scales and heterogeneous structure in geodynamic Earth models. *Science* **280**, 91–95.

Bunge, H.-P., Ricard, Y. & Matas, J. 2001 Non-adiabaticity in mantle convection. *Geophys. Res. Lett.* **28**, 879–882.

Bunge, H.-P., Hagelberg, C. & Travis, B. 2002 Mantle circulation models with variational data assimilation: inferring past mantle flow and structure from plate motion histories and seismic tomography. (In the press.)

Christensen, U. R. 1996 The influence of trench migration on slab penetration into the lower mantle. *Earth Planet. Sci. Lett.* **140**, 27–39.

Christensen, U. R. & Yuen, D. A. 1984 The interaction of a subducting lithospheric slab with a chemical or phase boundary. *J. Geophys. Res.* **89**, 4389–4402.

Dahlen, F. A., Hung, S. H. & Nolet, G. 2000 Frechet kernels for finite-frequency traveltimes. I. Theory. *Geophys. J. Int.* **141**, 157–174.

Davies, J. H. & Bunge, H.-P. 2001 Seismically 'fast' geodynamic mantle models. *Geophys. Res. Lett.* **28**, 73–76.

Davies, G. F. & Richards, M. A. 1992 Mantle convection. *J. Geol.* **100**, 151–206.

Dickenson, W. R. & Snyder, W. S. 1978 *Plate tectonics of the Laramide orogeny.* Geophysical Society of America Memoir Series, vol. 151, pp. 355–366.

Dziewonski, A. M. 1984 Mapping the lower mantle: determination of lateral heterogeneity in P velocity up to degree and order 6. *J. Geophys. Res.* **89**, 5929–5952.

Dziewonski, A. M., Hager, B. H. & O'Connell, R. J. 1977 Large-scale heterogeneities in the lower mantle. *J. Geophys. Res.* **82**, 239–255.

Farnetani, C. G. 1997 Excess temperature of mantle plumes: the role of chemical stratification across D''. *Geophys. Res. Lett.* **24**, 1583–1586.

Glatzmaier, G. A. 1988 Numerical simulations of mantle convection: time-dependent, three-dimensional, compressible, spherical shell. *Geophys. Astrophys. Fluid Dynam.* **43**, 223–264.

Glatzmaier, G. A. & Roberts, P. H. 1995 A three-dimensional self-consistent computer simulation of a geomagnetic field reversal. *Nature* **377**, 203–209.

Glatzmaier, G. A., Coe, R., Hongre, L. & Roberts, P. 1999 The role of the Earth's mantle in controlling the frequency of geomagnetic reversals. *Nature* **401**, 885–890.

Gordon, R. G. & Jurdy, D. M. 1986 Cenozoic global plate motions. *J. Geophys. Res.* **91**, 12 389–12 406.

Grand, S. P., van der Hilst, R. D. & Widiyantoro, S. 1997 Global seismic tomography: a snapshot of convection in the Earth. *GSA Today* **7**, 1–6.

Gurnis, M. & Davies, G. 1986*a* Mixing in numerical models of mantle convection incorporating plate kinematics. *J. Geophys. Res.* **91**, 6375–6395.

Gurnis, M. & Davies, G. F. 1986*b* Numerical study of high Rayleigh number convection in a medium with depth-dependent viscosity. *Geophys. J. R. Astr. Soc.* **85**, 523–541.

Hager, B. H. & Clayton, R. W. 1989 Constraints on the structure of mantle convection using seismic observations, flow models, and the geoid. In *Mantle convection: plate tectonics and global dynamics* (ed. W. R. Peltier), pp. 657–763. New York: Gordon & Breach.

Hager, B. H. & O'Connell, R. J. 1979 Kinematic models of large-scale flow in the Earth's mantle. *J. Geophys. Res.* **84**, 1031–1048.

Hofmann, A. W. 1997 Mantle geochemistry: the message from oceanic volcanism. *Nature* **385**, 219–229.

Jellinek, A. M., Gunnerman, H. M. & Richards, M. A. 2002 Plume capture by divergent plate motions: implications for the distribution of hotspots, geochemistry of mid-ocean ridge basalts, and heat flux at the core–mantle boundary. (In preparation.)

Johnson, S., Masters, T. G., Tackley, P. J. & Glatzmaier, G. A. 1993 How well can we resolve a convecting Earth with seismic data? (abstract). *Eos* **74**(43), 80. (Fall Meeting Suppl.)

Jordan, T. H. 1978 Composition and development of continental tectosphere. *Nature* **274**, 544–548.

Katsura, T. & Ito, E. 1989 The system Mg_2SiO_4–Fe_2SiO_4 at high pressures and temperatures: precise determination of stabilities of olivine, modified spinel and spinel. *J. Geophys. Res.* **94**, 15 663–15 670.

Kellogg, L. H., Hager, B. H. & van der Hilst, R. D. 1999 Compositional stratification in the deep mantle. *Science* **283**, 1881–1884.

Kennett, B. L. N., Widiyantoro, S. & van der Hilst, R. D. 1998 Joint seismic tomography for bulk sound and shear wave speed in the Earth's mantle. *J. Geophys. Res.* **103**, 12 469–12 493.

Komatitsch, D. & Tromp, J. 1999 Introduction to the spectral element method for three-dimensional seismic wave propagation. *Geophys. J. Int.* **139**, 806–822.

Kuang, W. L. & Bloxham, J. 1997 An Earth-like numerical dynamo model. *Nature* **389**, 371–374.

Li, X. D. & Romanowicz, B. 1996 Global mantle shear velocity model developed using nonlinear asymptotic coupling theory. *J. Geophys. Res.* **101**, 22 245–22 272.

Lithgow-Bertelloni, C. & Richards, M. A. 1998 The dynamics of Cenozoic and Mesozoic plate motions. *Rev. Geophys.* **36**, 27–78.

Masters, G., Jordan, T. H., Silver, P. G. & Gilbert, F. 1982 Aspherical Earth structure from fundamental spheroidal-mode data. *Nature* **298**, 609–613.

Masters, G., Johnson, S., Laske, G. & Bolton, H. 1996 A shear-velocity model of the mantle. *Phil. Trans. R. Soc. Lond.* A **354**, 1385–1410.

Meltzer, A. (and 11 others) 1999 USArray initiative. *GSA Today* **9**, 8–10.

Mitrovica, J. X. 1996 Haskell (1935) revisited. *J. Geophys. Res.* **101**, 555–569.

Murnaghan, F. D. 1951 *Finite deformation of an elastic solid*. Wiley.

Ricard, Y., Richards, M. A., Lithgow-Bertelloni, C. & Le Stunff, Y. 1993 A geodynamic model of mantle density heterogeneity. *J. Geophys. Res.* **98**, 21 895–21 909.

Richards, M. A. & Engebretson, D. C. 1992 Large-scale mantle convection and the history of subduction. *Nature* **355**, 437–440.

Richards, M. A., Bunge, H.-P. & Lithgow-Bertelloni, C. 2000 Mantle convection and plate motion history: toward general circulation models. In *The history and dynamics of global plate motions* (ed. M. A. Richards *et al.*). Geophysical Monograph Series, vol. 121, pp. 289–307. American Geophysical Union.

Richards, M. A., Yang, W.-S., Baumgardner, J. R. & Bunge, H.-P. 2001 The role of a low viscosity zone in stabilizing plate tectonics: implications for comparative terrestrial planetology. *Geochem. Geophys. Geosyst.* **2**, 1–16.

Ritsema, J. & van Heijst, H. J. 2000 Seismic imaging of structural heterogeneity in Earth's mantle: evidence for large-scale mantle flow. *Sci. Prog.* **83**, 243–259.

Sleep, N. H. 1990 Hotspots and mantle plumes: some phenomenology. *J. Geophys. Res.* **95**, 6715–6736.

Solheim, L. P. & Peltier, W. R. 1994 Avalanche effects in phase transition modulated thermal convection: a model of the Earth's mantle. *J. Geophys. Res.* **99**, 6997–7018.

Steinberger, B. & O'Connell, R. J. 1997 Changes of the Earth's rotation axis owing to advection of mantle density heterogeneities. *Nature* **387**, 169–173.

Tackley, P. J. 2000 Mantle convection and plate tectonics: toward an integrated physical and chemical theory. *Science* **288**, 2002–2007.

Tackley, P. J., Stevenson, D. J., Glatzmaier, G. A. & Schubert, G. 1993 Effects of an endothermic phase transition at 670 km depth on a spherical model of convection in Earth's mantle. *Nature* **361**, 699–704.

Tackley, P. J., Stevenson, D. J., Glatzmaier, G. A. & Schubert, G. 1994 Effects of multiple phase transitions in a three-dimensional spherical model of convection in Earth's mantle. *J. Geophys. Res.* **99**, 15 877–15 901.

Talagrand, O. 1997 Assimilation of observations: an introduction. *J. Meteorol. Soc. Jpn* **75**, 191–209.

Trompert, R. & Hansen, U. 1998 Mantle convection simulations with rheologies that generate plate-like behaviour. *Nature* **395**, 686–689.

Urey, H. C. 1956 The cosmic abundance of potassium, uranium and thorium and the heat balances of the Earth, the Moon and Mars. *Proc. Natl Acad. Sci. USA* **42**, 889–891.

van der Hilst, R. D. 1995 Complex morphology of subducted lithosphere in the mantle beneath the Tonga trench. *Nature* **374**, 154–157.

van der Hilst, R. D., Widiyantoro, S. & Engdahl, E. R. 1997 Evidence for deep mantle circulation from global tomography. *Nature* **386**, 578–584.

van der Lee, S. & Nolet, G. 1997 Seismic image of the subducted trailing fragments of the Farallon plate. *Nature* **386**, 266–269.

van der Voo, R., Spakman, W. & Bijwaard, H. 1999 Mesozoic subducted slabs under Siberia. *Nature* **397**, 246–249.

Williams, Q. 1997 The temperature contrast across D''. In *The core–mantle boundary region* (ed. M. Gurnis *et al.*). Geodynamic Series, vol. 28, pp. 73–82. American Geophysical Union.

Wunsch, C. 1996 *The ocean circulation inverse problem*. Cambridge University Press.

Zhong, S. & Gurnis, M. 1994 Role of plates and temperature dependent viscosity in phase change dynamics. *J. Geophys. Res.* **99**, 15 903–15 917.

Zhong, S. & Gurnis, M. 1996 Interaction of weak faults and non-newtonian rheology produces plate tectonics in a 3D model of mantle flow. *Nature* **383**, 245–247.

Zhong, S., Zuber, M. T., Moresi, L. & Gurnis, M. 2000 Role of temperature-dependent viscosity and surface plates in spherical shell models of mantle convection. *J. Geophys. Res.* **105**, 11 063–11 082.